Resveratrol Activates Autophagic Cell Death in Prostate Cancer Cells via Downregulation of STIM1 and the mTOR Pathway

Senthil Selvaraj,[1,2]* Yuyang Sun,[1] Pramod Sukumaran,[1] and Brij B. Singh[1]*

[1]Department of Basic Sciences, School of Medicine and Health Sciences, University of North Dakota, Grand Forks, North Dakota
[2]Qatar Cardiovascular Research Center, Qatar Foundation, Doha, Qatar

Resveratrol (RSV), a natural polyphenol, has been suggested to induce cell cycle arrest and activate apoptosis-mediated cell death in several cancer cells, including prostate cancer. However, several molecular mechanisms have been proposed on its chemopreventive action, the precise mechanisms by which RSV exerts its anti-proliferative effect in androgen-independent prostate cancer cells remain questionable. In the present study, we show that RSV activates autophagic cell death in PC3 and DU145 cells, which was dependent on stromal interaction molecule 1 (STIM1) expression. RSV treatment decreases STIM1 expression in a time-dependent manner and attenuates STIM1 association with TRPC1 and Orai1. Furthermore, RSV treatment also decreases ER calcium storage and store operated calcium entry (SOCE), which induces endoplasmic reticulum (ER) stress, thereby, activating AMPK and inhibiting the AKT/mTOR pathway. Similarly, inhibition of SOCE by SKF-96365 decreases the survival and proliferation of PC3 and DU145 cells and inhibits AKT/mTOR pathway and induces autophagic cell death. Importantly, SOCE inhibition and subsequent autophagic cell death caused by RSV was reversed by STIM1 overexpression. STIM1 overexpression restored SOCE, prevents the loss of mTOR phosphorylation and decreased the expression of CHOP and LC3A in PC3 cells. Taken together, for the first time, our results revealed that RSV induces autophagy-mediated cell death in PC3 and DU145 cells through regulation of SOCE mechanisms, including downregulating STIM1 expression and trigger ER stress by depleting ER calcium pool.
© 2015 The Authors. Molecular Carcinogenesis, published by Wiley Periodicals, Inc.

Key words: resveratrol; SOCE; TRPC1; orai1; STIM1; ER stress; autophagy; prostate cancer

INTRODUCTION

Prostate cancer (PCa) is the most commonly diagnosed cancer in the male population of western descent and is the leading cause of cancer-related death in men who are older than 65 [1,2]. Anti-androgen therapy is remarkable in the early stages of prostate tumors development since the growth is completely dependent on androgens. However, in majority of cases, the tumor progress to androgen insensitive stage where androgen is not required for their growth, for which currently no successive therapy is available [3]. Therefore, a better understanding of the mechanism(s) and identification of novel target molecules that control the androgen insensitive prostate cancer cell proliferation and the development of novel therapeutic drugs, are essentially needed in the near future.

Prostate epithelial cells express a large number of Ca^{2+} permeable channels that are required to regulate different cellular functions including proliferation and differentiation. Loss of Ca^{2+} homeostasis modulation, could be at least in part, the mechanisms where the prostate cancer epithelial cells become resistant to apoptotic stimuli which ultimately leads to uncontrolled proliferation and invasion [4,5]. Recent studies have suggested that intracellular Ca^{2+} as well as Ca^{2+} channels play a major role in PCa progression [6,7]. For example, double knockdown of α1D-adrenergic receptor (α1D–AR) and transient receptor potential vanilloid type 1 (TRPV1) inhibit noradrenaline-induced PC3 cell proliferation by suppressing Ca^{2+} influx, and reducing the activation of phospholipase C (PLC), protein kinase C (PKC), and extracellular signal-regulated kinase 1/2 (ERK1/2) pathways [8]. Similarly, other studies have shown that calcium influx through TRPC6, TRPV6, TRPM8, and T-type Ca^{2+} channels participate in the proliferation of PCa cells [9–12]. On the other hand, massive Ca^{2+} influx via the store

operated Ca^{2+} entry (SOCE) mechanism induces apoptosis-mediated cell death in several cancer cells [5,13]. Therefore, studying the Ca^{2+} permeable channels and its downstream signaling pathways may be effective in the identification of novel drug targets that could be used for tumor regression.

SOCE is an important cellular mechanism that ensure the optimal refilling of endoplasmic reticulum (ER)/sarcoplasmic reticulum (SR) Ca^{2+} stores, activation of several Ca^{2+} mediated pro and anti-survival mechanisms, and gene transcription. In excitable and non-excitable cells, SOCE is mediated by store operated Ca^{2+} channels (SOCs) which are located in the plasma membrane and depletion of ER Ca^{2+} stores activates the SOCs-mediated Ca^{2+} influx (known as SOCE). Interestingly, changes in ER Ca^{2+} levels and SOCs function play a crucial role in the establishment of an androgen-independent apoptosis resistance phenotype of PCa [5,14,15]. Members of TRPC family particularly, TRPC1 and TRPC4 have been identified as the promising molecular candidates for SOCs in androgen-dependent LNCaP cells [16,17] and notably, recent studies have identified two other molecular components of SOCs, Orai1 and STIM1 [18,19]. Stromal interaction molecule 1 (STIM1) is a single transmembrane ER/SR resident protein with NH2-terminal Ca^{2+} binding EF hand directed to the lumen of the ER that functions as a signal transducer from ER to SOCs. Upon store depletion, STIM1 translocates to plasma membrane where it interacts with TRPC1 and/or Orai1 to initiate SOCE [18]. Several studies have shown that SOCE and SOCs are involved in cell cycle progression, proliferation, and migration [9,20], but its role in PCa as well as downstream signaling mechanism is still not yet established.

Dietary polyphenols are the most abundant natural antioxidants in the human food and recent reports suggested the efficacy of natural antioxidants in controlling the growth and migration of various cancers [21]. Studies have suggested that dietary intake of natural antioxidants could halt cancer progression. Resveratrol (trans-3,4′,5-trihydroxystilbene; RSV), a natural polyphenolic antioxidant is found in a wide variety of fruits including grapes, raspberries, and other plants. Several in vitro and in vivo studies have suggested the growth inhibitory efficacy of RSV in several types of cancer cells, notably leukemia, breast, colon, liver, lung, thyroid, and other epithelial cancers [21,22]. Importantly, the anticarcinogenic effect of RSV in PCa has been shown and it is widely associated with changes in the expression of cell cycle regulating molecules such as, cyclin A, cyclin E, cdc2, and Rb. Several other studies have also noticed that RSV inhibits the proliferation of androgen-dependent and independent prostate cancer cell lines by activating the apoptotic pathway [23,24]. Moreover, RSV regulates the expression of PSA (prostate specific antigen) by an androgen receptor (AR)-dependent and AR-

independent mechanism, and also RSV enhances the effect of anti-AR drug bicalutamide [23–25]. However, the role of SOCE in RSV-mediated anticancer effect and the precise mechanisms by which RSV exerts its anti-proliferative effect in androgen-independent PCa cell lines remain unanswered. Thus, we have investigated whether SOCE is involved in prostate cancer cell proliferation and does RSV affect cell viability through SOCs-dependent Ca^{2+} pathways. To address this, we have used two androgen-independent prostate epithelial cells PC3 and DU145 along with control RWPE-1 cells. The results from our study suggest that RSV inhibits prostate cancer proliferation by downregulating STIM1, thereby, inhibiting SOCE and initiating autophagic cell death.

MATERIALS AND METHODS

Cell Culture Reagents and Transfection

Control prostate cell line RWPE1 (CRL 11609) and PCa cell line DU145 (HTB-81) and PC3 (CRL1435) cells were obtained from the American Type Culture Collection (Manassas, VA). Cells were cultured in their respective medium along with various supplements as suggested by ATCC. Cells were maintained at 37°C with 95% humidified air and 5% CO_2 and were passaged as needed. Culture medium was changed twice weekly and cells were maintained in complete media, until reaching 90% confluence. For overexpression, HA-STIM1 was used and 5 μg of plasmid DNA was transfected using Lipofectamine 2000 in Opti-MEM medium as per supplier's instructions and assayed after 24 h.

Cell Proliferation and Cell Viability Assays

The 10,000 cells were plated in 96-well plates and synchronized by stimulating with 10% FBS, then pulsed with BrdU for 2 h before BrdU incorporation was measured as per manufacturer's instructions (Roche). For viability assays, cells were seeded on 96-well plates at a density of 0.5×10^5 cells/well. Cell viability was measured by using the Vybrant MTT cell proliferation assay kit (Invitrogen-Molecular Probes, Eugene, OR). Absorbance was read at 570 nm (630 nm as a reference) on a microplate reader (Molecular Devices). Cell viability was expressed as a percentage of the control culture.

Immunoprecipitation and Western Blotting

Immunoprecipitations were carried out as described earlier [26]. RIPA buffer was used to prepare the total cell lysates. Following stimulation, cells were lysed with RIPA buffer and used for immunoprecipitation. Protein concentrations were determined using the Bradford reagent (Bio-Rad Laboratories Inc., CA) and 25–50 μg of proteins were resolved in 4–12% NuPAGE gels, followed by Western blotting with the desired antibodies. Crude membrane was prepared from DU145 and PC3 cells as described previously [27]. Proteins

were resolved on 4–12% Bis-Tris gels (Invitrogen), transferred to PVDF membranes and probed with respective antibodies. Peroxidase-conjugated respective secondary antibodies were used to label the proteins. The proteins were detected by enhanced chemiluminescence detection kit (SuperSignal West Pico; Pierce, Invitrogen-Molecular Probes, Eugene, OR). Antibodies that were used in this study are from Cell Signaling Technology (Danvers, MA) and Alomone Labs (TRPC1 and Orai1 antibodies). All other reagents used were of molecular biology grade obtained from Sigma chemicals unless mentioned otherwise.

Confocal Images

PC3 and DU145 cells were transiently transfected with GFP-LC3 by using Lipofectamine 2000 in Opti-MEM medium as described by the manufacturer. After 24 h, cells were treated with RSV for 24 h and then fixed in 4% formaldehyde for 10 min. Cells were then washed thrice with PBS and images were collected using a MRC1024-krypton/argon laser scanning confocal equipped with a Zeiss LSM 510 Meta photomicroscope.

Calcium Measurements

Cells were incubated with $2\,\mu M$ fura-2 (Molecular Probes) for 45 min, washed twice with Ca2+ free SES (Standard External Solution, includes: 10 mM HEPES, 120 mM NaCl, 5.4 mM KCl, 1 mM MgCl2, 10 mM glucose, pH 7.4) buffer. For fluorescence measurements, the fluorescence intensity of fura-2-loaded control cells was monitored with a CCD camera-based imaging system (Compix) mounted on an Olympus XL70 inverted microscope equipped with an Olympus $40\times$ (1.3 NA) objective. A monochrometer dual wavelength enabled alternative excitation at 340 and 380 nm, whereas the emission fluorescence was monitored at 510 nm with an Okra Imaging camera (Hamamatsu, Japan). The images of multiple cells collected at each excitation wavelength were processed using the C imaging, PCI software (Compix, Inc., Cranbery, PA), to provide ratios of fura-2 fluorescence from excitation at 340 nm to that from excitation at 380 nm (F340/F380). Fluorescence traces shown represent $[Ca^{2+}]i$ values that are averages from at least 30–40 cells and are a representative of results obtained in at least 3–4 individual experiments.

Electrophysiology

For patch clamp experiments, coverslips with cells were transferred to the recording chamber and perfused with an external Ringer's solution of the following composition (mM): NaCl, 145; CsCl, 5; MgCl2, 1; CaCl2, 1; Hepes, 10; Glucose, 10; pH 7.3 (NaOH). Whole cell currents were recorded using an Axopatch 200B (Axon Instruments Inc., CA). The patch pipette had resistances between 3 and 5 M after filling with the standard intracellular solution that contained the following (mM): cesium methane

sulfonate, 150; NaCl, 8; Hepes, 10; EGTA, 10; pH 7.2 (CsOH). With a holding potential 0 mV, voltage ramps ranging from -100 to $+100$ mV and 100 ms duration were delivered at 2 s intervals after whole cell configuration was formed. Currents were recorded at 2 kHz and digitized at 5–8 kHz. pClamp 10.1 software was used for data acquisition and analysis. Basal leak were subtracted from the final currents and average currents are shown. All experiments were carried out under room temperature.

Statistics

Data analysis was performed using Origin 7.0 (OriginLab). Statistical comparisons were made using Student's t-test (2-tailed). Experimental values are expressed as mean $\pm$ SEM. Differences in the mean values were considered to be significant at $P < 0.05$ or $P < 0.01$ or $P < 0.001$.

RESULTS

Ca^{2+}-induced regulation of cell proliferation and survival in prostate cancer cells. Ca^{2+} not only functions as a second messenger, but have also been shown to be critical for cell proliferation and migration [7]. Importantly, increase in Ca^{2+} signaling have been shown to activate the immediate early genes that are responsible for inducing resting cells to re-enter the cell cycle and has been suggested to be a target for anticancer therapy [28,29]. We thus evaluated the role of increasing Ca^{2+} concentration in prostate cancer cell proliferation and/or their survival. Importantly, increasing extracellular Ca^{2+} concentration showed a dose-dependent increase in cell survival in prostate cancerous cells (DU145 and PC3) (Figure 1A and B). Although in the presence of increasing extracellular Ca^{2+}, RWPE1 cells also showed a moderate increase in cell survival, the amount of increase in cell proliferation was relatively less when compared with cancer cells (data not shown). We next evaluated if cell proliferation was also increased under these conditions and again both DU145 and PC3 cells showed a significant increase in BrdU incorporation in the presence of increasing extracellular Ca^{2+} (Figure 1C and D). Overall, these data suggest that increasing extracellular Ca^{2+} is important for the increase of cell proliferation of PCa cells.

Agonist-stimulated Ca^{2+} entry has been suggested to play an essential role in regulating cell survival and increasing cell proliferation. Importantly, in non-excitable cells both Orai1 and TRPC1 has been shown to be important for Ca^{2+} entry that are activated by agonist-mediated ER store depletion, a phenomenon termed as SOCE. Thus, we next evaluated the expression of these Ca^{2+} entry channels in prostate cells. Although, no change in TRPC1 or Orai1 levels were observed in control and PCa cells, a decrease in STIM1 levels was observed in control RWPE1 cells, when compared with PCa cells (DU145 and PC3)
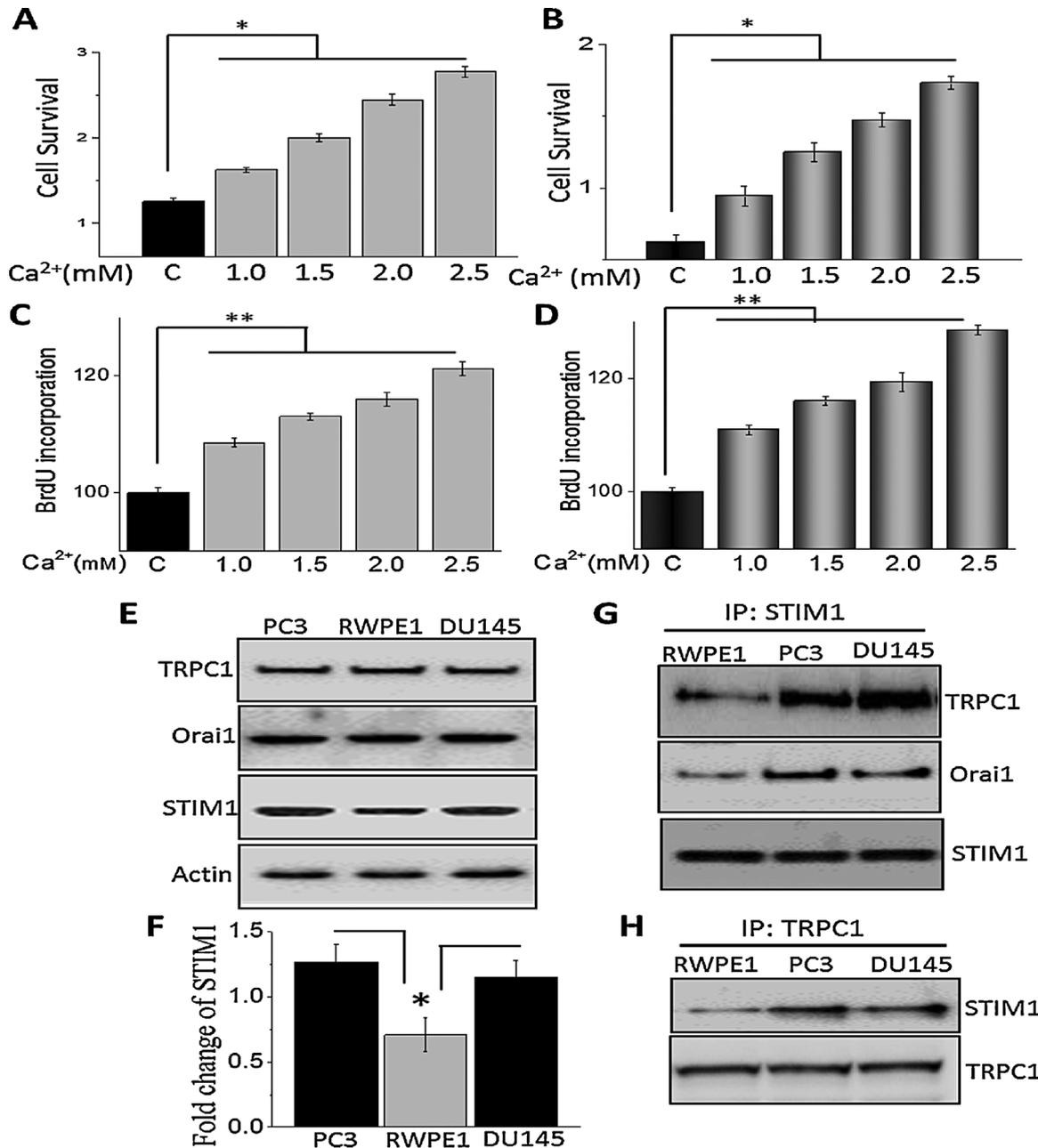
Figure 1. Calcium-induced regulation of cell proliferation and survival in prostate cancer cells. (A and B) PC3 and DU145 cells were treated with different concentration of Ca^{2+} for 24 h. Cell survival was measured using MTT assay as described in Materials and Methods section. Values are expressed as mean ± SEM ($n = 4$). *$P < 0.05$ versus respective control cells. Bar diagram showing the relative absorbance at 450 nm of PC3 and DU145 cells after BrDU incorporation under various concentration of calcium are shown in (C and D). Results are expressed as mean ± SEM ($n = 4$) *$P < 0.05$ and **$P < 0.01$ versus respective control. (E) Western blotting was showing the expression of TRPC1, Orai1, and STIM1 in PC3, RWPE1, and DU145 cells. (F) Densitometric quantitation for normalized STIM1 relative to β-actin is shown. Values represent mean ± SEM from three to four independent experiments (*$P < 0.05$). (G and H) Whole-cell lysates were prepared and immunoprecipitation was performed with anti-STIM1 or anti-TRPC1 antibody as described in Materials and Methods section. The immunoprecipitates were subjected to immunoblot analysis with anti-STIM1, anti-TRPC1, and anti-Orai1 antibodies.

($P < 0.05$; Figure 1E and F). STIM1 has been recently identified as a key Ca^{2+} entry regulator that is present in the ER and sense ER Ca^{2+} levels [19]. Furthermore, upon store depletion STIM1 has been shown to interact with TRPC1 and Orai1 channels to initiate Ca^{2+} entry via SOCE that could be essential for cell proliferation and survival [18]. Importantly, the functional interaction between STIM1 and TRPC1/Orai1 was also increased in PCa cells when compared with control RWPE1 cells (Figure 1G and H). Overall, these data indicate that Ca^{2+}-mediated increase in cell proliferation and survival of PCa cells, is perhaps

due to increased STIM1 expression. In addition, increase in STIM1–TRPC1/Orai1 interaction could also facilitate Ca^{2+} entry via the SOCE mechanism that could promote cell survival and proliferation of PCa cells.

RSV inhibits cell proliferation and survival of PCa cells by downregulating STIM1. RSV, an antioxidant agent mainly concentrated in red grapes, has been shown to decrease the risk of many cancers [21]; however, the mechanism is not well defined. Thus, we next evaluated if addition of RSV decreases cell proliferation and survival of PCa cells. Cells treated with RSV for 24 h showed a dose-dependent decrease in the cell survival of prostate cancerous cells (PC3 and DU145) (Figure 2A and B). Similarly, cell proliferation was also decreased and both PC3 and DU145 cells showed a significant decrease in BrdU incorporation (Figure 2C and D). Data presented in Figure 1 suggest that increase in STIM1 expression and its interaction with TRPC1/Orai1 could be critical for increased cell proliferation/survival of PCa cells. Therefore, we also evaluated the expression of TRPC1, Orai1, and STIM1 in control and RSV-treated PCa cells. Importantly, no change in the overall or surface expression of TRPC1 or Orai1 was observed upon RSV treatment. In contrast a decrease in total STIM1 levels was observed in RSV-treated cancer cells ($P < 0.05$; Figure 2E–H). We and others have previously shown that upon store-depletion, STIM1 is targeted to the ER–PM junctions where it interacts with TRPC1 channels [30,31]. Thus, co-immunoprecipitation experiments using STIM1 antibodies were performed in control and store-depleted conditions. Addition of thapsigargin (Tg, SERCA pump blocker), showed an increase in STIM1–TRPC1 interaction in both PC3 and DU145 cells, which was also decreased in RSV treatment cells (Figure 2I). These data suggest that RSV inhibit STIM1–TRPC1 functional interaction that could inhibit Ca^{2+} entry and induce cell death in PCa cells.

Store-mediated Ca^{2+} entry is inhibited upon RSV treatment in PCa cells. Data presented thus far indicate that Ca^{2+} is essential for the proliferation/survival of PCa cells and RSV treatment not only inhibits STIM1 expression, but also inhibits Tg-induced association between TRPC1 and STIM1. Furthermore, as TRPC1 is activated via STIM1, and this association is important for SOC-mediated Ca^{2+} entry, we next evaluated if SOCE is altered upon RSV treatment. To evaluate SOC-mediated Ca^{2+} entry, ER Ca^{2+} stores were depleted by the addition of thapsigargin (Tg, $2\,\mu M$). Importantly, in the absence of extracellular Ca^{2+} the increase in $[Ca^{2+}]_i$ evoked by Tg (first peak) was significantly decreased in both PC3 and DU145 cells following RSV treatment, when compared with untreated cells (Figure 3A and B). Addition of external Ca^{2+} (1 mM), which initiates SOC-mediated Ca^{2+} entry, was also decreased in RSV treated PC3 and DU145 cells (Figure 3A and B) indicating that RSV

treatment inhibits SOCE, which could be critical for decreasing cell proliferation/survival.

To establish the identity of the SOC channel, electrophysiological recordings were performed in PCa cells. In PC3 cells, addition of Tg induced an inward current which was non-selective and reversed between 0 and -5 mV ($P < 0.05$; Figure 3C, D, and F). The currents shown in Figure 3C were recorded at a holding potential of -80 mV and I/Vs curves were developed using a ramp protocol where current density was evaluated at various membrane potential and plotted. Importantly, the channel properties were similar to those previously observed with TRPC1 channels [32], suggesting that TRPC1 could contribute to the endogenous SOC-mediated Ca^{2+} entry channel in PC3 cells. Similar results were also obtained with DU145 cells and the Tg-induced inward currents were similar as observed with PC3 cells (data not shown), also the I/V curves were similar between the two cells (Figure 3E). Also, SKF 96365, a non-specific TRPC channel blocker was used that showed a decrease in these inward currents in both PC3 and DU145 cells (data not shown). Importantly, addition of RSV significantly decreased SOC currents in both PC3 and DU145 cells without altering the current–voltage (I–V) relationship (Figure 3C–F). Collectively, these results suggest that RSV decreases ER Ca^{2+} by diminishing SOC-mediated Ca^{2+} entry, which could lead to the activation of the UPR in these cells that together would induce cell death.

RSV treatment induces ER stress followed by the inhibition of the AKT/mTOR pathway. To understand the mechanism(s) of RSV-mediated decrease in cell survival, we investigated the unfolded protein response (UPR) as loss of ER–Ca^{2+} that has been shown to induce ER stress [33]. UPR markers (GRP78 and CHOP) were upregulated at the protein levels in RSV-treated cells, whereas no change in GRP94 was observed (Figure 4A). Quantification of GRP78 is shown in Figure 4C ($P < 0.05$). Furthermore, RSV was previously shown to induce autophagy, thus we next evaluated the induction of autophagy in control and RSV-treated cancer cells. Importantly, in both PC3 and DU145 cells, RSV treatment showed an increase in LC3B-II, but did not show an increase in Beclin1 ($P < 0.05$; Figure 4B and C), suggesting that perhaps the autophagy induced by RSV is independent of Beclin1. In addition, $100\,\mu M$ RSV treatment resulted in accumulation of GFP-LC3 puncta in PC3 and DU145 cells; however, lower dose of RSV, $10\,\mu M$ failed to show a significant accumulation of GFP-LC3 when compared with control untreated cells (Figure 4D and E). Since the RSV-induced autophagy was independent of Beclin1, we next investigated if it was mediated via the mTOR pathway. Furthermore, Ca^{2+} entry has been shown to activate the AKT/ mTOR pathway, which is essential for inhibition of cell death. Importantly, RSV treatment attenuated the activation of mTOR, a kinase that regulates cell
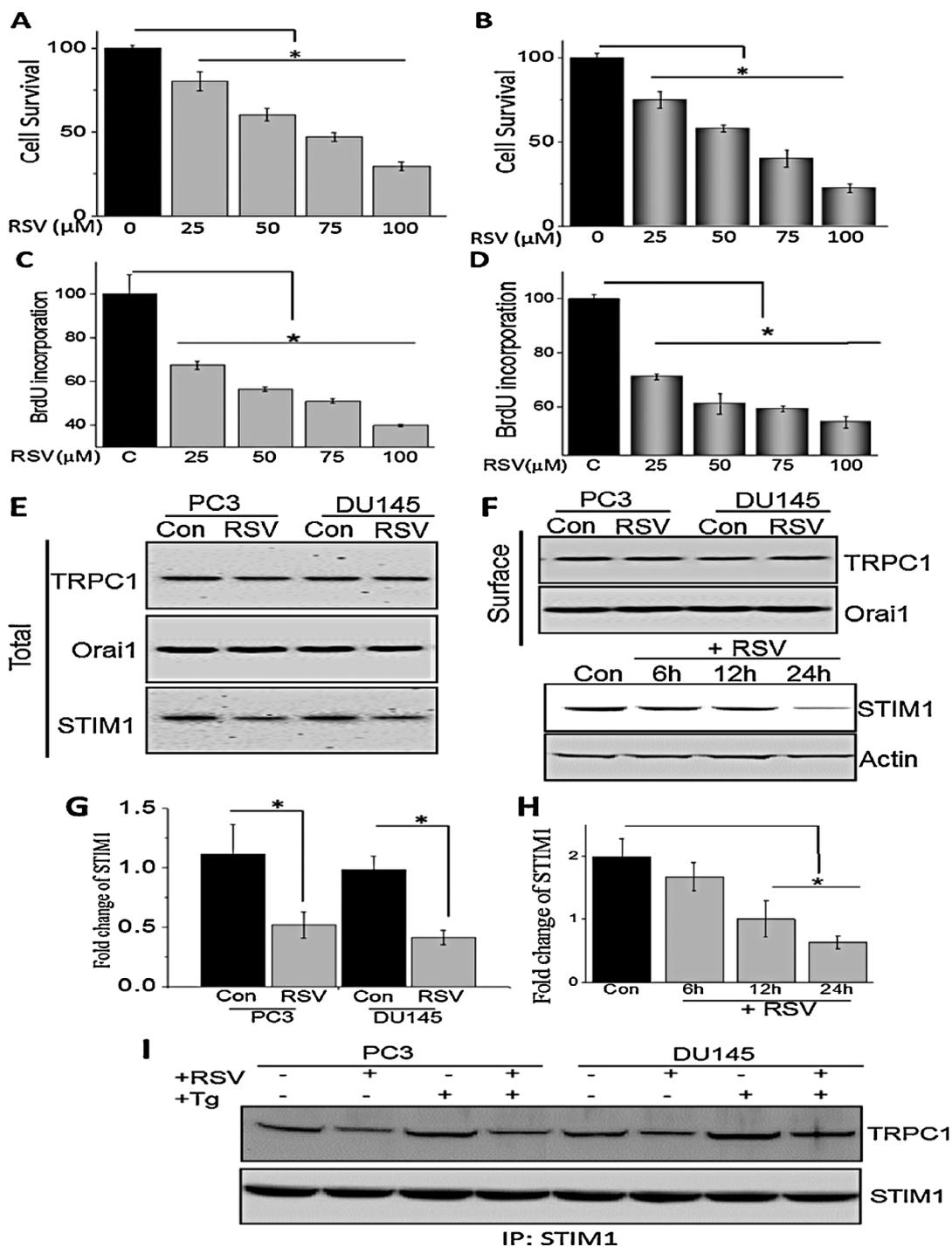
Figure 2. Resveratrol inhibits cell proliferation and survival of prostate cancer cells by downregulating STIM1: (A and B) PC3 and DU145 cells were treated with different RSV concentrations (dissolved in ethanol) for 24 h. Cell survival was measured using MTT assay as described in Materials and Methods section. Values are expressed as mean $\pm$ SEM ($n = 4$). $^*P < 0.05$ versus untreated control cells. Bar diagram showing the relative absorbance at 450 nm of PC3 and DU145 cells after BrDU incorporation under various concentration of RSV for 24 h are shown in (C and D). Values are expressed as mean $\pm$ SEM ($n = 4$). $^*P < 0.05$ versus untreated control cells. (E) PC3 and DU145 cells were treated with vehicle control or RSV for 24 h, lysed and proteins were subjected to SDS–PAGE followed by Western blotting with respective antibodies as labeled in the figure. (F) PC3 and DU145 cells were treated with 100 μM RSV for 24 h. Crude membrane was prepared and proteins were subjected to SDS–PAGE followed by Western blotting with TRPC1 and Orai1 antibodies. (F) Cells were treated with 100 μM RSV and cells were harvested at 0, 6, 12, or 24 h after RSV treatment. Cell lysates were resolved and analyzed by Western blotting. Antibodies used are labeled and actin was used as loading control. (G and H) Histogram represents the relative intensity of STIM1 normalized to β-actin. Values represent mean $\pm$ SEM from three to four independent experiments ($^*P < 0.05$). (I) PC3 and DU145 cells were treated with RSV or Tg in various conditions, lysed and proteins were subjected to SDS–PAGE followed by Western blotting with respective antibodies.
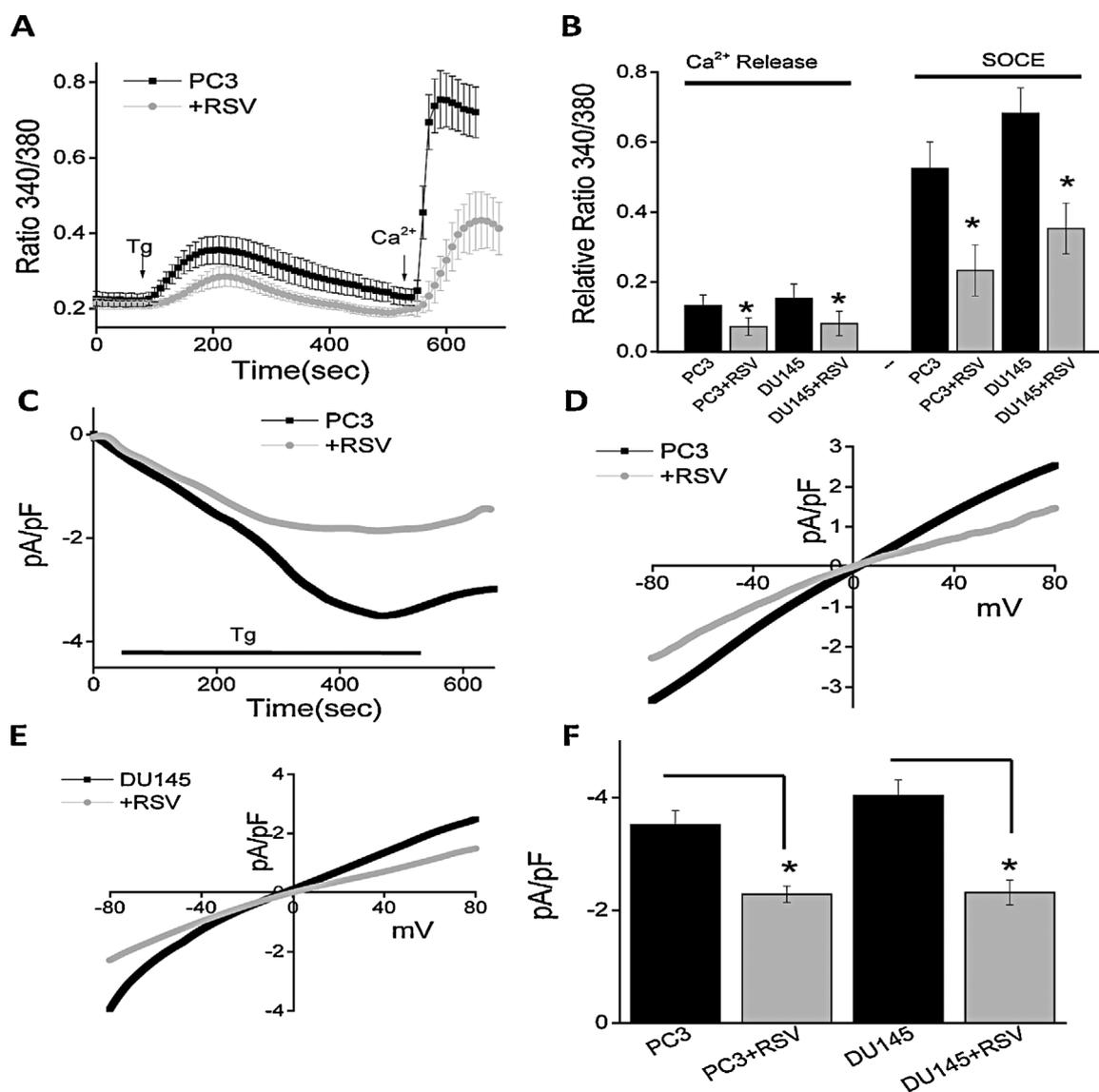
Figure 3. Store-mediated Ca^{2+} entry is inhibited upon RSV treatment in prostate cancer cells: (A) Ca^{2+} imaging was performed in control and in the presence of RSV (100 μM) for 24 h in PC3 cells. Analog plots of the fluorescence ratio (340/380) from an average of 40–60 cells are shown. (B) Quantification (mean ± SD) of fluorescence ratio (340/380). $^*P < 0.05$) versus control. (C) RSV treatment decreased SOCE currents in PC3 cells. Average IV curves under conditions control and RSV treatment are shown in (D). (E) RSV treatment changed IV curves of SOCE currents in DU145 cells. Average (8–10 recordings) current intensity at −80 mV under these conditions is shown in (F).

survival, in both PC3 and DU145 cells (Figure 4F). Activation of p70S6K and S6ribo that are downstream of mTOR were also inhibited in the presence of RSV (Figure 4F). Finally, RSV treatment also significantly decreased AKT1 phosphorylation (AKT^{473}) without affecting total AKT1 levels in PCa cells (Figure 4F). Quantification of phospho-mTOR, phospho-AMPKα, and phospho-AKT^{473} were shown in Figure 4G ($P < 0.05$). These results strongly suggest that RSV-mediated loss of Ca^{2+} influx could be essential for the activation of the protective AKT1/mTOR activation in PCa cells.

Decreasing Ca^{2+} entry in PCa cells also induce cell death. To better understand the link between Ca^{2+} influx and cell survival, we inhibited SOCE. Addition of SKF96365 that has been shown to block SOC-mediated Ca^{2+} entry [34], significantly decreased Tg-induced Ca^{2+} entry in PC3 cells (Figure 5A and B). Similar results were also obtained with DU145 cells where SKF96365 treatment inhibited SOC-mediated Ca^{2+} entry (data not shown). Importantly, increasing SKF96365 concentration significantly decreased cell survival in both DU145 and PC3 cells (Figure 5C and D). Similarly, cell proliferation was also decreased
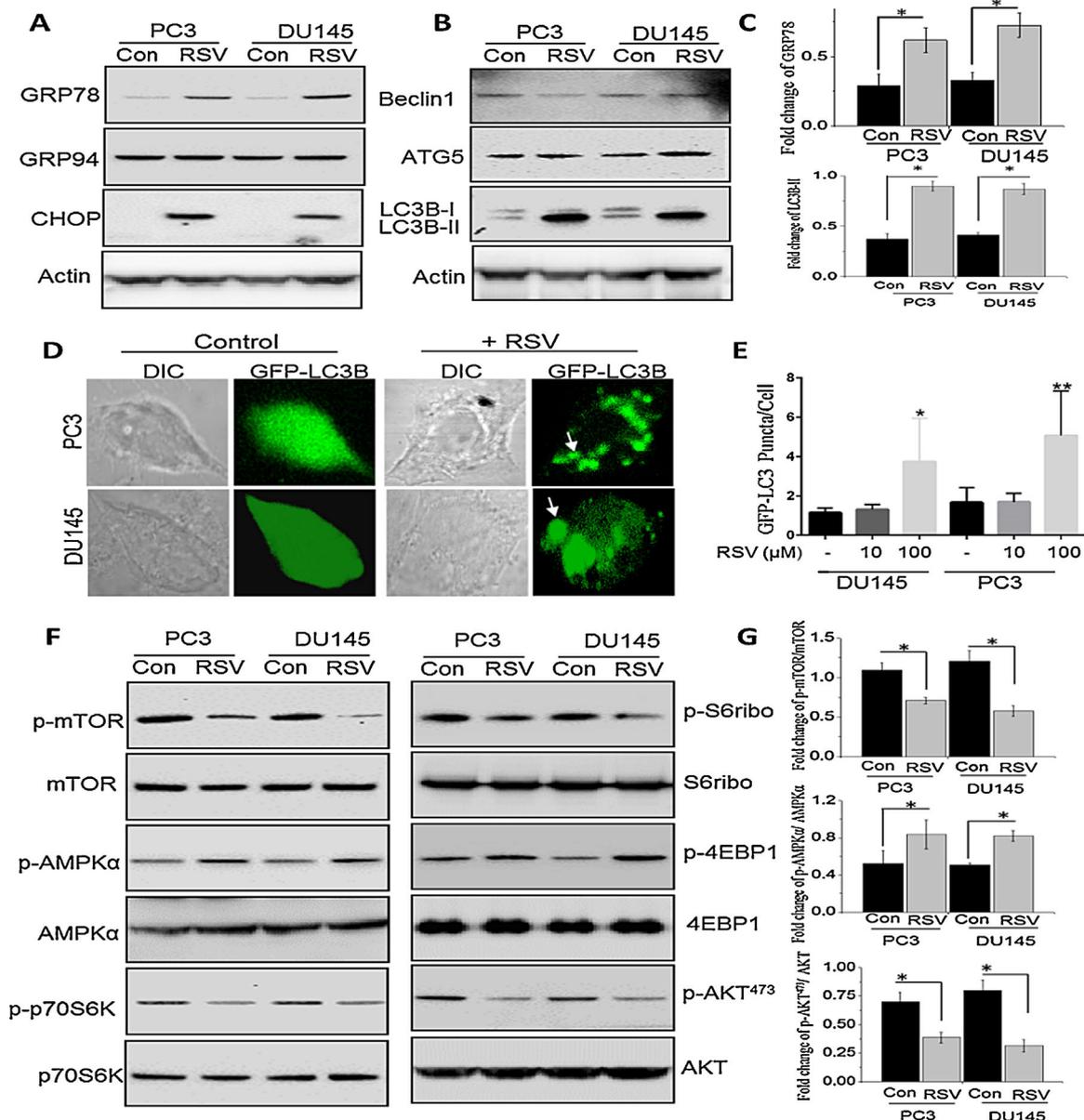
Figure 4. RSV treatment in prostate cancer cells induces ER stress and autophagy via inhibiting the mTOR/AKT pathway: (A) Western blot images showing the expression of unfolded protein response (UPR) markers (GRP78, GRP94, and CHOP) in the prostate cancer cells after 100 μM RSV treatment for 24 h. (B) Western blot images showing the expression of autophagy protein markers Beclin1, ATG5, LC3B in control, and RSV-treated cells. (C) Histogram represents the relative intensity of GRP78 and LC3B normalized to β-actin. Values represent mean ± SEM from three to four independent experiments ($^*P < 0.05$). (D and E) GFP-LC3 expressing PC3 and DU145 cells were treated with RSV for 24 h. Quantitation shown on the right represents mean ± SEM. GFP-positive puncta per cell from three independent experiments ($^*P < 0.05$ and $^{**}P < 0.01$). (F) Western blot images showing the phosphorylation of mTOR, AMPKα, p70S6K, S6ribo, 4EBP1, and AKT (Cell Signaling Technology, MA) in both PC3 and DU145 cells after 100 μM RSV treatment for 24 h. (G) Histogram represents the relative intensity of phospho-mTOR, phospho-AMPKα, and phospho-AKT normalized to their respective total proteins. Values represent mean ± SEM from three to four independent experiments ($^*P < 0.05$).

under these conditions and again both DU145 and PC3 cells showed a significant decrease in BrdU incorporation in the presence of increasing SKF96365 (Figure 5E and F). Consistent with these data, SKF96365 treatment also showed an increase in LC3A/B in PC3 and DU145 cells ($P < 0.05$; Figure 5G and H); however, the effect in PC3 cells was more prominent. Our data presented in Figure 4 also showed that the AKT/mTOR pathway was important, and SKF96365 treatment inhibits the activation of mTOR and AKT1 in both PC3 and DU145 cells (Figure 5I). Together, these data suggest that inhibition of Ca^{2+} entry leads to decreased cell proliferation/survival of PCa cells via the inhibition of the AKT/mTOR pathway.
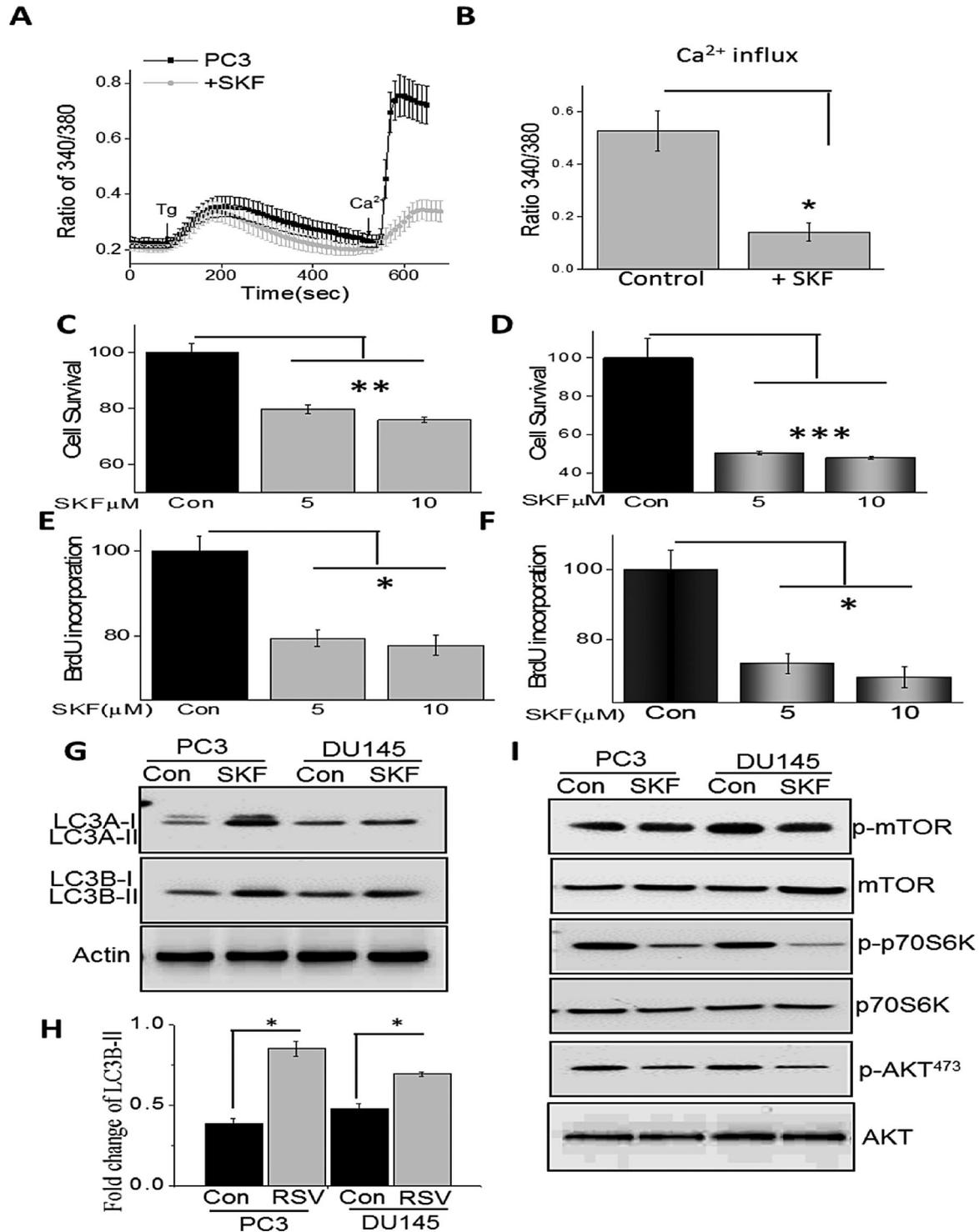
Figure 5. Decreasing Ca²⁺ entry in prostate cancer cells also induce cell death: (A) Ca²⁺ imaging was performed in control and in the presence of SKF 96365 in PC3 cells. Analog plots of the fluorescence ratio (340/380) from an average of 40–60 cells are shown. (B) Quantification (mean ± SD) of fluorescence ratio (340/380). $^{*}P < 0.05$ versus control. MTT assays under various concentration of SKF 96365 treated conditions for 24 h in PC3 and DU145 cells are shown in (C and D). Bar diagram showing the relative absorbance at 450 nm of PC3 and DU145 cells after BrDU incorporation and various SKF concentrations are shown in (E and F). Each bar gives the mean ± SEM of four separate experiments. $^{*}P < 0.05$, $^{**}P < 0.01$, and $^{***}P < 0.001$, respectively. Western blot images showing the expression of autophagy protein markers LC3A and LC3B, mTOR, p70S6K, and AKT in both PC3 and DU145 cells after 10 μM SKF 96365 treatment for 24 h (G–I). Histogram represents the relative intensity of LC3B normalized to β-actin. Values represent mean ± SEM from three to four independent experiments ($^{*}P < 0.05$).

Restoration of STIM1 expression reverts RSV-mediated inhibition of cell proliferation and survival of PCa cells. To further establish that indeed RSV-mediated loss in Ca^{2+} influx (due to loss of STIM1 expression) is essential for cell death, we overexpressed STIM1 in PC3 cells. Expression of STIM1 plasmid showed increased STIM1 expression, whereas no increase in control actin levels was observed (Figure 6A). Importantly, RSV-dependent inhibition of SOC-mediated Ca^{2+} entry was also restored in cells that overexpress STIM1 (Figure 6B and C). Finally, both cell survival and cell proliferation were restored in cells that overexpress STIM1 and were treated with various doses of RSV (Figure 6D and E). Furthermore, phosphorylation of mTOR was also restored in STIM1 overexpressing cells that were treated with RSV (Figure 6F and G). Consistent with these results, both LC3A and CHOP expression that induces cell death were decreased in STIM1 overexpressing cells that were treated with RSV (Figure 6F and G). Overall, these results suggest that increase in STIM1 expression restores RSV-dependent loss in Ca^{2+} entry and inhibits RSV-mediated inhibition of cell proliferation and survival. These results also suggest a mechanism as why some cancer cells are resistant to cell death upon RSV treatment—as a threshold of STIM1
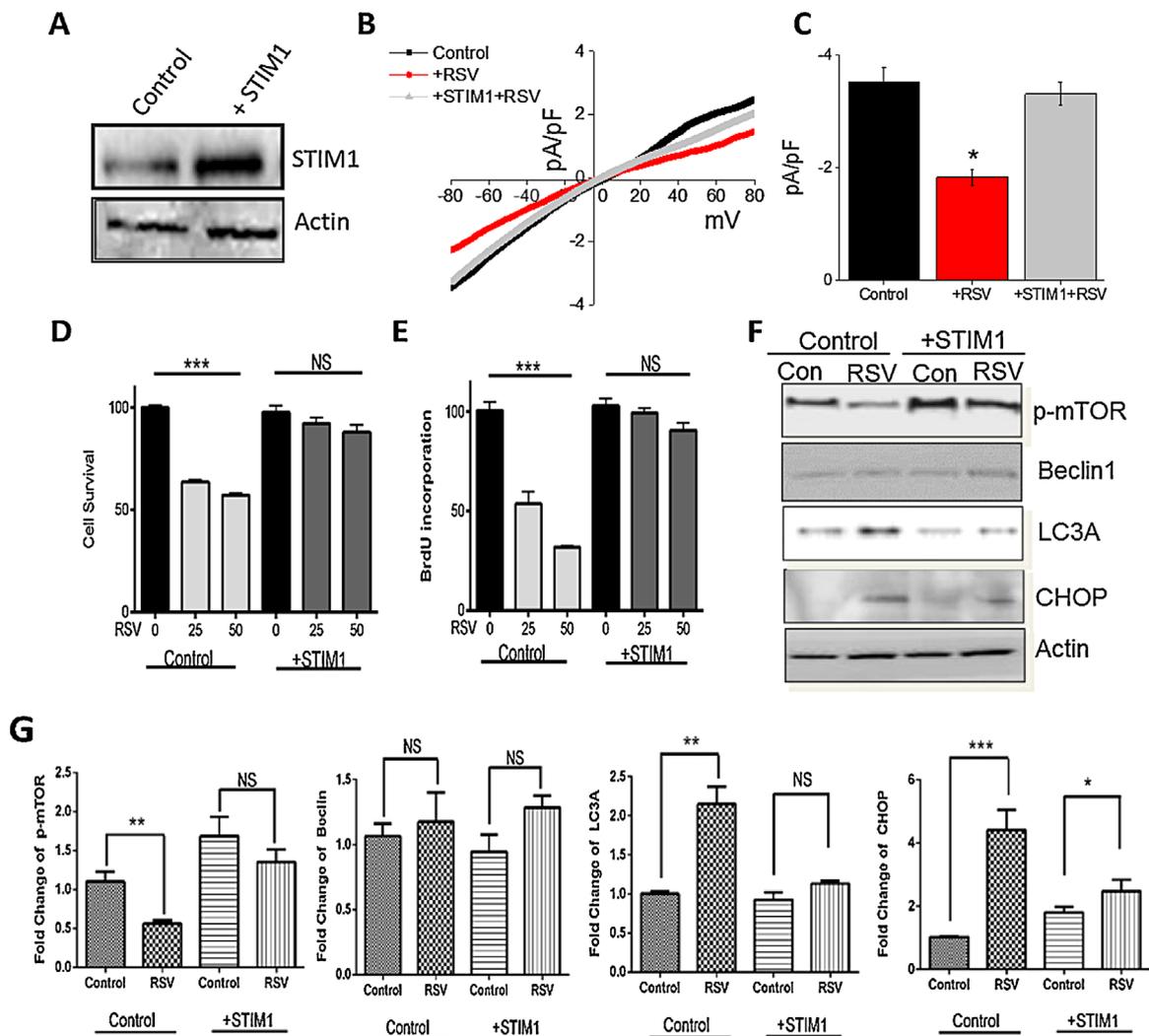

Figure 6. Restoration of STIM1 expression reverts resveratrol-mediated inhibition of cell proliferation and survival of prostate cancer cells: (A) Western blot image showing the overexpression of STIM1 in PC3 cells. (B) STIM1 overexpression restored IV curve of SOCE currents in PC3 cells. Average (8–10 recordings) current intensity at -80 mV under these conditions is shown in (C). MTT assays under various concentration of RSV conditions in control and STIM1 overexpressed PC3 cells are shown in (D). Bar diagram showing the relative absorbance at 450 nm of control and STIM1 overexpressed PC3 cells after BrDU incorporation under various concentration of RSV are shown in (E). Each bar gives the mean ± SEM of four separate experiments. $^{***}P < 0.001$. (F) Western blot images showing the expressions of p-mTOR, Beclin1, CHOP, and β-Actin in control and STIM1 overexpressed PC3 cells with or without RSV treatment. Histogram represents the relative intensity of phospho-mTOR, Beclin1, LC3A, and CHOP normalized to β-actin. Values represent mean ± SEM from three to four independent experiments ($^{*}P < 0.05$, $^{**}P < 0.01$, and $^{***}P < 0.001$).

expression is perhaps critical for RSV-mediated cells death.

DISCUSSION

Cytosolic Ca^{2+} mediates several cellular signaling pathways that are related to proliferation, differentiation, and migration of tumor cells [20]. The Ca^{2+} influx from the extracellular space and Ca^{2+} release from the intracellular sources determine the cytosolic Ca^{2+} concentration. Previously, we have shown that increase in serum Ca^{2+}/Mg^{2+} ratio promotes PCa epithelial cell proliferation by activating TRPM7, which functions as an endogenous MagNuM channel in PCa cells. Furthermore, decrease in the Ca^{2+}–Mg^{2+} ratio, facilitated Ca^{2+} entry and led to an increase in cell proliferation of cancer cells [35]. Therefore, changes in the expression or function of Ca^{2+} channels could affect the cytosolic Ca^{2+} homeostasis and its dependent cellular process, such as proliferation and survival. Moreover, the role of Ca^{2+} in autophagic cell death has also been recently elucidated in cancer cells and studies have also shown that the cytosolic Ca^{2+} as a major regulator of both basal and induced autophagy [36].

Interestingly, the anti-carcinogenic activity of dietary polyphenol, RSV has been widely studied both in vitro and in vivo tumor models, including PCa [21,22,25]. It is well known that RSV induces cell cycle arrest, inhibits cell proliferation, and activates apoptosis in androgen-independent PCa cells [24,37]. The present study, in conjunction with previous studies, demonstrates that RSV inhibits PCa cell proliferation and induces autophagy in PC3 and DU145 cells. Several mechanisms have been shown to mediate the anti-proliferative effects of RSV in PCa cells; however, the precise mechanism of RSV-mediated growth inhibition and the involvement of Ca^{2+} remain unclear. Several phase I and phase II clinical trials are currently in progress at the National Institute of Health (http:/clinicaltrials.gov) for therapeutic effect of RSV against several cancer types including patients with colon cancer and lymphoma [38]; however, there are no results from PCa patients. Understanding the downstream signaling mechanisms of resveratrol-induced cell death may facilitate the development of additional therapeutic targets for the androgen-independent PCa prevention and treatment. The results of this study demonstrate that STIM1 is an important target of RSV for inhibiting cell proliferation and to activate ER stress-mediated autophagic cell death in androgen-independent PCa epithelial cells.

Store operated Ca^{2+} entry is the predominant Ca^{2+} influx mechanism in PCa cells. Substantial progress has been made throughout the last two decades in the elucidation of the key players of SOCE and mechanisms responsible for SOCE activation in both excitable and non-excitable cells. Importantly, these studies have identified an involvement of TRPCs and/or Orai1 channels in SOCE. Indeed, Stim1 has also been identified recently as the molecular switch that modulates SOC channels and its significance in SOCE has been elucidated in androgen-dependent PCa cells [15,39]. Nevertheless, it is unclear about the targets and mechanisms by which SOCE exerts its effects on cell function and survival in androgen-independent PCa cells. The data presented here show that SOCE is increased in androgen-independent cells, DU145, and PC3 when compared with normal prostate epithelial cells, RWPE1. MTT assay and BrdU incorporation demonstrated that external Ca^{2+} mediates the survival and proliferation of DU145 and PC3 cells. These results are consistent with other reports showing that the proliferative effect of external Ca^{2+} and SOCE in cancer cell [6,20,40]. Moreover, ER Ca^{2+} depletion and subsequent Ca^{2+} influx through SOCE have been previously shown to be critical in promoting growth arrest and apoptosis of PCa epithelial cells [4,13].

To address the role of SOCs, we studied the expression of TRPC1, Orai1, and STIM1 level in normal and PCa cells. Our results clearly showed that there were no significant differences in the protein levels of TRPC1 and Orai1; whereas STIM1 levels were increased in cancer cells when compared with control cells. Moreover, the interaction of STIM1 with TRPC1 and Orai1 was also increased in cancer cells. STIM1 is an ER resident protein, monitors the Ca^{2+} level in the ER by luminal EF Ca^{2+} binding domain, and translocates upon store depletion to plasma membrane to activate SOCE channels [19]. These results suggest that STIM1 interaction with either Orai1 or TRPC1 causes an increase in SOCE in androgen-independent PCa cells. Studies have also shown that molecular components of SOCs, particularly Orai1, TRPC1, and STIM1 seem to play a crucial role in cell proliferation and migration in several human cancers notably, breast, renal, cervical, and lung cancers indicating that inhibition of SOCE suppresses tumorigenicity [41,42]. The data presented here supports the hypothesis that Ca^{2+} entry through SOCE channels may activate the Ca^{2+}-dependent signaling process such as proliferation and survival that are critical for carcinogenesis, in androgen-independent PCa cells.

Our current study demonstrates that RSV prevents cell proliferation and induces cell death in a dose-dependent manner. Interestingly, $100\,\mu M$ RSV for 24 h abolishes both ER Ca^{2+} release as well as SOCE in DU-145 and PC-3 cells by decreasing STIM1 expression. However, the expression pattern of TRPC1 and Orai1 was not affected upon RSV treatment, but, RSV treatment decreases the STIM1–TRPC1 interaction upon store depletion. Previous study has shown that alteration in the expression of SOCs, particularly Orai1, contributes to the increased resistance of PCa cells toward induction of apoptosis. Our data

substantiate the recent study indicating that STIM1 may play an important role in the development of PCa and inhibition of its expression induces cell death in PC3 cells [43]. A growing number of studies have also shown that blockade or knockdown of STIM1 or TRPC1 significantly inhibits the proliferation and migration of cancer cell [41,43]. However, the underlying mechanisms seem to involve the reduction of SOCE upon STIM1 knockdown which suppress the carcinogenic cytosolic Ca^{2+} signaling in cancer cells. Our data are quite promising in which we found that RSV induces cell death by decreasing STIM1 expression and subsequent SOCE in androgen-independent DU145 and PC3 cells. Several pieces of our data also support the conclusion that RSV inhibits PCa cell proliferation by reducing SOCE. For example, RSV decreases the expression of STIM1 and dissociates the association of TRPC1–STIM1 and Orai1–STIM1 in DU145 and PC3 cells. Inhibition of SOCE by SKF-96365 decreases the survival and proliferation of DU145 and PC3 cells, whereas, restoration of SOCE via STIM1 overexpression attenuated the RSV-induced cell death. Overall, these results suggested that STIM1 is a primary target of RSV for mediating its anti-carcinogenic activity. However, it should be noted that RSV also regulates several other mechanisms including ER stress and autophagy via STIM1 and SOCE-dependent manner.

RSV was shown to induce pro-apoptotic ER stress in several cancer cells [44,45]. However, the exact mechanisms that proceed the cancer cells to ER stress under RSV treatment is not yet unveiled. Depletion of ER Ca^{2+} is known to cause ER stress and the current study has shown that RSV decreases SOCE, a vital mechanisms for ER Ca^{2+} store refilling, which ultimately could result in the depletion of ER Ca^{2+} store in DU145 and PC3 cells. As expected, Ca^{2+} release from the internal stores was significantly decreased upon RSV treatment. The shortage of ER Ca^{2+} may cause a deterioration in the protein folding in the lumen of the ER and cause ER stress [33,46]. Consistent with this, we found that RSV significantly induced ER stress, such as upregulation of GRP78/Bip and CHOP/GADD153 protein. Induction of GRP78, also called Bip, may be a pro-survival mechanism of the cells, since it assists in the folding of nascent unfolded proteins, prevents the Ca^{2+} efflux from the ER to the cytosol, and alleviates ER stress-induced apoptotic stimuli [47]. However, if the ER stress persists, cells induce the expression of CHOP, a unique transcription factor that mediates the ER stress-induced apoptosis. Induction or overexpression of CHOP sensitizes cells to ER stress-mediated apoptosis whereas knockdown or deletion protects the cell from apoptosis [48]. However, our results have shown that RSV treatment in DU145 and PC3 cells resulted in increased autophagy. Based on our results, we may hypothesize that treatment of PCa cells with RSV will lead to ER Ca^{2+} depletion and subsequent ER stress, which itself might also be a trigger for autophagy.

Autophagy is a catabolic process for the degradation and recycling of macromolecules and organelles, which is activated during stress conditions. Autophagy has a dual role in cancer cells, likely this could be a survival or cell death mechanism. For example, autophagy-mediated cell death is the predominant cell death mechanism in response to certain anti-cancer drugs [49,50]. On the contrary, autophagy activates pro-survival mechanisms that attenuates anti-cancer drug-induced apoptosis [51]. Several natural compounds, such as curcumin, paclitaxel, oridonin, quercetin, and fisetin, have been shown to induce autophagy-mediated cell death in a variety of tumor cells [52,53]. Thus, dietary natural compounds that induce autophagy may be of potential use as anti-cancer agents. Several studies have also shown that RSV is capable of inducing autophagy in different cancer cell line models [52,53]. Scarlatti and colleagues reported that RSV activates non-canonical Beclin-1-independent autophagy in MCF-7 cells [54]. Similarly, RSV promotes autophagic cell death in chronic myelogenous leukemia cells through both JNK-mediated p62 expression and AMPK activation, and stimulates both apoptosis and autophagy in ovarian carcinoma cells [55,56]. Opipari et al., reported that RSV inhibited cell proliferation and induced autophagocytosis in ovarian carcinoma cell lines [57]. Several studies have further shown that RSV induces apoptosis-mediated cell death in a variety of cancer cells including PCa cell lines [25,52,53]. In this study, we observed that in androgen-independent PCa cells, RSV activates ER stress-mediated autophagy that was independent of Beclin1. LC3 is widely considered the marker for autophagy since during autophagosome formation, LC3 (cytosolic microtubule associated protein light chain 3) is processed and conjugated with phosphatidylethanolamine (PE) and inserted into autophagic vesicle membranes [58,59]. The expression and accumulation of LC3 was robustly increased in RSV-treated cells, albeit only at higher doses, which confirms that RSV induced autophagic flux.

Several signaling pathways are known to regulate autophagy including the ERK, PI3K class I and II, and mTOR. The mTOR signaling pathways regulate various cellular process including autophagy through coordinating several signaling molecules such as S6K, 4EBP-1, and AKT. The mTOR/AKT pathway is an important signaling mechanism that regulates different cellular process including cell survival, proliferation, apoptosis, and autophagy [60,61]. Indeed it has been shown that the mTOR/AKT pathway is critical for prostate tumor growth and survival, especially when the PTEN, a tumor suppressor gene, is mutated [62]. Moreover, overexpression and uncontrolled activation of AKT have been identified in several human cancers including PCa [63,64]. Similarly, inactivation of mTOR pathway is shown to inhibit PCa cell growth, migration, and invasion [63].

Interestingly, the role of mTOR in SOCE activation has been elucidated recently in tuberous sclerosis complex-related tumor development. The study has shown that mTORC1 activates SOCE, and augmented SOCE by hyperactive mTORC1-STIM1 cascade may contribute to the benign nature of tuberous sclerosis complex (TSC)-related tumors. Interestingly, mTORC1 inhibitor, rapamycin suppressed the SOCE by decreasing the expression of STIM1 in tuberous sclerosis complex 2(TSC2)-deficient MEF cells [65]. Hence, it is suggested that to develop a drug that can inhibit both mTOR and other signaling molecules, PI3K/AKT would be an effective strategy in treating PCa. Consistent with these studies, we observed that RSV treatment activates the AMPK and inhibits the mTOR/AKT phosphorylation. The results suggest that RSV induces autophagy through regulating mTOR/AKT pathways. However, the RSV-induced autophagy was abolished in STIM1 overexpressed PC3 cells. The STIM1 overexpression reverts the RSV-induced SOCE suppression, ER stress, and cell death which indicate that RSV targets SOCE via suppressing STIM1 and deplete ER store causes ER stress-induced autophagic cell death in androgen-independent PCa cells. Moreover, the signaling pathways by which RSV regulates autophagy induction and exerts its anti-carcinogenic effects are far from being completely elucidated. Although several studies suggest that increase in intracellular Ca^{2+} may contribute to anti-carcinogenic effect, this has never been clearly proven. Nevertheless, further investigations are needed to elucidate the molecular mechanisms by which STIM1 regulates PCa cell proliferation and survival.

In conclusion, SOCE is crucially involved in the survival and proliferation of androgen-independent PCa cell lines, DU145 and PC3, and RSV treatment attenuates SOCE and induces autophagy-mediated cell death. The mechanisms involve altered expression of STIM1 and subsequent SOCE influx which cause an ER stress response in DU145 and PC3 cells. ER stress further potentiates the autophagy-mediated cell death through regulating mTOR/AKT pathways. To the best of our knowledge, this is the first report that RSV induces autophagic cell death by regulating the function of STIM1 and subsequent SOCE.

ACKNOWLEDGMENTS

REFERENCES

1. Jemal A, Siegel R, Ward E, Hao Y, Xu J, Thun MJ. Cancer Statistics, 2009. CA Cancer J Clin 2009;59:225–249.
2. DeSantis CE, Lin CC, Mariotto AB, et al. Cancer treatment and survivorship statistics, 2014. CA Cancer J Clin 2014;64:252–271.
3. Denis LJ, Griffiths K. Endocrine treatment in prostate cancer. Semin Surg Oncol 2000;18:52–74.
4. Prevarskaya N, Skryma R, Shuba Y. Ca2+ homeostasis in apoptotic resistance of prostate cancer cells. Biochem Biophys Res Commun 2004;322:1326–1335.
5. Vanoverberghe K, Vanden Abeele F, Mariot P, et al. Ca2+ homeostasis and apoptotic resistance of neuroendocrine-differentiated prostate cancer cells. Cell Death Differ 2004;11:321–330.
6. Shapovalov G, Skryma R, Prevarskaya N. Calcium channels and prostate cancer. Recent Pat Anticancer Drug Discov 2013;8:18–26.
7. Flourakis M, Prevarskaya N. Insights into Ca2+ homeostasis of advanced prostate cancer cells. Biochim Biophys Acta 2009;1793:1105–1109.
8. Morelli MB, Amantini C, Nabissi M, et al. Cross-talk between alpha1D-adrenoceptors and transient receptor potential vanilloid type 1 triggers prostate cancer cell proliferation. BMC Cancer 2014;14:921.
9. Thebault S, Flourakis M, Vanoverberghe K, et al. Differential role of transient receptor potential channels in Ca2+ entry and proliferation of prostate cancer epithelial cells. Cancer Res 2006;66:2038–2047.
10. Zhang L, Barritt GJ. Evidence that TRPM8 is an androgen-dependent Ca2+ channel required for the survival of prostate cancer cells. Cancer Res 2004;64:8365–8373.
11. Fixemer T, Wissenbach U, Flockerzi V, Bonkhoff H. Expression of the Ca2+-selective cation channel TRPV6 in human prostate cancer: A novel prognostic marker for tumor progression. Oncogene 2003;22:7858–7861.
12. Weaver EM, Zamora FJ, Puplampu-Dove YA, Kiessu E, Hearne JL, Martin-Caraballo M. Regulation of T-type calcium channel expression by sodium butyrate in prostate cancer cells. Eur J Pharmacol 2015;749:20–31.
13. Skryma R, Mariot P, Bourhis XL, et al. Store depletion and store-operated Ca2+ current in human prostate cancer LNCaP cells: Involvement in apoptosis. J Physiol 2000;527:71–83.
14. Li N, Zheng L, Lin P, Danielpour D, Pan Z, Ma J. Overexpression of Bax induces down-regulation of store-operated calcium entry in prostate cancer cells. J Cell Physiol 2008;216:172–179.
15. Flourakis M, Lehen'kyi V, Beck B, et al. Orai1 contributes to the establishment of an apoptosis-resistant phenotype in prostate cancer cells. Cell Death Dis 2010;1:e75.
16. Vanden Abeele F, Lemonnier L, Thebault S, et al. Two types of store-operated Ca2+ channels with different activation modes and molecular origin in LNCaP human prostate cancer epithelial cells. J Biol Chem 2004;279:30326–30337.
17. Vanden Abeele F, Shuba Y, Roudbaraki M, et al. Store-operated Ca2+ channels in prostate cancer epithelial cells: Function, regulation, and role in carcinogenesis. Cell Calcium 2003;33:357–373.
18. Liao Y, Erxleben C, Abramowitz J, et al. Functional interactions among Orai1, TRPCs, and STIM1 suggest a STIM-regulated heteromeric Orai/TRPC model for SOCE/Icrac channels. Proc Natl Acad Sci USA 2008;105:2895–2900.
19. Lewis RS. The molecular choreography of a store-operated calcium channel. Nature 2007;446:284–287.
20. Prevarskaya N, Skryma R, Shuba Y. Calcium in tumour metastasis: New roles for known actors. Nat Rev Cancer 2011;11:609–618.
21. Aluyen JK, Ton QN, Tran T, Yang AE, Gottlieb HB, Bellanger RA. Resveratrol: Potential as anticancer agent. J Diet Suppl 2012;9:45–56.
22. Delmas D, Lancon A, Colin D, Jannin B, Latruffe N. Resveratrol as a chemopreventive agent: A promising molecule for fighting cancer. Curr Drug Targets 2006;7:423–442.
23. Hudson TS, Hartle DK, Hursting SD, et al. Inhibition of prostate cancer growth by muscadine grape skin extract and

resveratrol through distinct mechanisms. Cancer Res 2007;67:8396–8405.

24. Kim YA, Rhee SH, Park KY, Choi YH. Antiproliferative effect of resveratrol in human prostate carcinoma cells. J Med Food 2003;6:273–280.

25. Jasinski M, Jasinska L, Ogrodowczyk M. Resveratrol in prostate diseases—a short review. Cent European J Urol 2013;66:144–149.

26. Pani B, Ong HL, Brazer SC, et al. Activation of TRPC1 by STIM1 in ER-PM microdomains involves release of the channel from its scaffold caveolin-1. Proc Natl Acad Sci USA 2009;106:20087–20092.

27. Singh BB, Lockwich TP, Bandyopadhyay BC, et al. VAMP2-dependent exocytosis regulates plasma membrane insertion of TRPC3 channels and contributes to agonist-stimulated Ca2+ influx. Mol Cell 2004;15:635–646.

28. Berridge MJ, Lipp P, Bootman MD. The versatility and universality of calcium signalling. Nat Rev Mol Cell Biol 2000;1:11–21.

29. Berridge MJ, Bootman MD, Roderick HL. Calcium signalling: Dynamics, homeostasis and remodelling. Nat Rev Mol Cell Biol 2003;4:517–529.

30. Yuan JP, Zeng W, Huang GN, Worley PF, Muallem S. STIM1 heteromultimerizes TRPC channels to determine their function as store-operated channels. Nat Cell Biol 2007;9:636–645.

31. Pani B, Ong HL, Liu X, Rauser K, Ambudkar IS, Singh BB. Lipid rafts determine clustering of STIM1 in endoplasmic reticulum-plasma membrane junctions and regulation of store-operated Ca2+ entry (SOCE). J Biol Chem 2008;283:17333–17340.

32. Liu X, Cheng KT, Bandyopadhyay BC, et al. Attenuation of store-operated Ca2+ current impairs salivary gland fluid secretion in TRPC1(−/−) mice. Proc Natl Acad Sci USA 2007;104:17542–17547.

33. Kaufman RJ. Stress signaling from the lumen of the endoplasmic reticulum: Coordination of gene transcriptional and translational controls. Genes Dev 1999;13:1211–1233.

34. Derouiche S, Warnier M, Mariot P, et al. Bisphenol A stimulates human prostate cancer cell migration remodelling of calcium signalling. Springerplus 2013;2:54.

35. Sun Y, Selvaraj S, Varma A, Derry S, Sahmoun AE, Singh BB. Increase in serum Ca2+/Mg2+ ratio promotes proliferation of prostate cancer cells by activating TRPM7 channels. J Biol Chem 2013;288:255–263.

36. Hoyer-Hansen M, Bastholm L, Szyniarowski P, et al. Control of macroautophagy by calcium, calmodulin-dependent kinase kinase-beta, and Bcl-2. Mol Cell 2007;25:193–205.

37. Benitez DA, Pozo-Guisado E, Alvarez-Barrientos A, Fernan-dez-Salguero PM, Castellon EA. Mechanisms involved in resveratrol-induced apoptosis and cell cycle arrest in prostate cancer-derived cell lines. J Androl 2007;28:282–293.

38. Bishayee A. Cancer prevention and treatment with resveratrol: From rodent studies to clinical trials. Cancer Prev Res 2009;2:409–418.

39. Kondratskyi A, Yassine M, Slomianny C, et al. Identification of ML-9 as a lysosomotropic agent targeting autophagy and cell death. Cell Death Dis 2014;5:e1193.

40. Borowiec AS, Bidaux G, Pigat N, Goffin V, Bernichtein S, Capiod T. Calcium channels, external calcium concentration and cell proliferation. Eur J Pharmacol 2014;739:19–25.

41. Chen J, Luan Y, Yu R, Zhang Z, Zhang J, Wang W. Transient receptor potential (TRP) channels, promising potential diagnostic and therapeutic tools for cancer. Biosci Trends 2014;8:1–10.

42. Roberts-Thomson SJ, Peters AA, Grice DM, Monteith GR. ORAI-mediated calcium entry: Mechanism and roles, diseases and pharmacology. Pharmacol Ther 2010;127:121–130.

43. Gu P, Zhou YB, Yang DR, Shan YX, Xue BX. Inhibition of stromal interaction molecule 1 and the expression of apoptosis-related proteins in prostate cancer PC-3 cells. Zhonghua Nan Ke Xue 2014;20:225–228.

44. Wang FM, Galson DL, Roodman GD, Ouyang H. Resveratrol triggers the pro-apoptotic endoplasmic reticulum stress response and represses pro-survival XBP1 signaling in human multiple myeloma cells. Exp Hematol 2011;39:999–1006.

45. Huang TT, Lin HC, Chen CC, et al. Resveratrol induces apoptosis of human nasopharyngeal carcinoma cells via activation of multiple apoptotic pathways. J Cell Physiol 2011;226:720–728.

46. Ma Y, Hendershot LM. The unfolding tale of the unfolded protein response. Cell 2001;107:827–830.

47. Li J, Lee AS. Stress induction of GRP78/BiP and its role in cancer. Curr Mol Med 2006;6:45–54.

48. Schonthal AH. Pharmacological targeting of endoplasmic reticulum stress signaling in cancer. Biochem Pharmacol 2013;85:653–666.

49. Yang ZJ, Chee CE, Huang S, Sinicrope FA. The role of autophagy in cancer: Therapeutic implications. Mol Cancer Ther 2011;10:1533–1541.

50. White E. Deconvoluting the context-dependent role for autophagy in cancer. Nat Rev Cancer 2012;12:401–410.

51. Guo XL, Li D, Hu F, et al. Targeting autophagy potentiates chemotherapy-induced apoptosis and proliferation inhibition in hepatocarcinoma cells. Cancer Lett 2012;320:171–179.

52. Mukhtar E, Adhami VM, Khan N, Mukhtar H. Apoptosis and autophagy induction as mechanism of cancer prevention by naturally occurring dietary agents. Curr Drug Targets 2012;13:1831–1841.

53. Zhang X, Chen LX, Ouyang L, Cheng Y, Liu B. Plant natural compounds: Targeting pathways of autophagy as anti-cancer therapeutic agents. Cell Prolif 2012;45:466–476.

54. Scarlatti F, Maffei R, Beau I, Codogno P, Ghidoni R. Role of non-canonical Beclin 1-independent autophagy in cell death induced by resveratrol in human breast cancer cells. Cell Death Differ 2008;15:1318–1329.

55. Kartal M, Saydam G, Sahin F, Baran Y. Resveratrol triggers apoptosis through regulating ceramide metabolizing genes in human K562 chronic myeloid leukemia cells. Nutr Cancer 2011;63:637–644.

56. Puissant A, Robert G, Fenouille N, et al. Resveratrol promotes autophagic cell death in chronic myelogenous leukemia cells via JNK-mediated p62/SQSTM1 expression and AMPK activation. Cancer Res 2010;70:1042–1052.

57. Opipari AW, Jr., Tan L, Boitano AE, Sorenson DR, Aurora A, Liu JR. Resveratrol-induced autophagocytosis in ovarian cancer cells. Cancer Res 2004;64:696–703.

58. Mizushima N, Yoshimori T. How to interpret LC3 immuno-blotting. Autophagy 2007;3:542–545.

59. Kabeya Y, Mizushima N, Yamamoto A, Oshitani-Okamoto S, Ohsumi Y, Yoshimori T. LC3, GABARAP and GATE16 localize to autophagosomal membrane depending on form-II formation. J Cell Sci 2004;117:2805–2812.

60. Sun H, Wang Z, Yakisich JS. Natural products targeting autophagy via the PI3K/Akt/mTOR pathway as anticancer agents. Anticancer Agents Med Chem 2013;13:1048–1056.

61. Beauchamp EM, Platanias LC. The evolution of the TOR pathway and its role in cancer. Oncogene 2013;32:3923–3932.

62. Persad S, Attwell S, Gray V, et al. Inhibition of integrin-linked kinase (ILK) suppresses activation of protein kinase B/Akt and induces cell cycle arrest and apoptosis of PTEN-mutant prostate cancer cells. Proc Natl Acad Sci USA 2000;97:3207–3212.

63. Bitting RL, Armstrong AJ. Targeting the PI3K/Akt/mTOR pathway in castration-resistant prostate cancer. Endocr Relat Cancer 2013;20:R83–R99.

64. Majumder PK, Sellers WR. Akt-regulated pathways in prostate cancer. Oncogene 2005;24:7465–7474.

65. Peng H, Liu J, Sun Q, et al. MTORC1 enhancement of STIM1-mediated store-operated Ca2+ entry constrains tuberous sclerosis complex-related tumor development. Oncogene 2013;32:4702–4711.